AIAA 96-2240
Hypervelocity Heat-Transfer Measurements in an Expansion Tube

Brian R. Hollis, John N. Perkins
North Carolina State University
Raleigh, NC

19th AIAA Advanced Measurement and Ground Testing Technology Conference

June 18-20, 1996/New Orleans, LA

Hypervelocity Heat-Transfer Measurements in an Expansion Tube

Brian R. Hollis* and John N. Perkins†
Department of Mechanical and Aerospace Engineering
North Carolina State University
Raleigh, NC 27695-7910

ABSTRACT

A series of experiments has been conducted in the NASA HYPULSE Expansion Tube, in both CO_2 and air test gases, in order to obtain data for comparison with computational results and to assess the capability for performing hypervelocity heat-transfer studies in this facility. Heat-transfer measurements were made in both test gases on 70 deg sphere-cone models and on hemisphere models of various radii. HYPULSE freestream flow conditions in these test gases were found to be repeatable to within ±3-10%, and aerothermodynamic test times of 150 μsec in CO_2 and 125 μsec in air were identified. Heat-transfer measurement uncertainty was estimated to be ±10-15%. Comparisons were made with computational results from the non-equilibrium Navier-Stokes solver NEQ2D. Measured and computed heat-transfer rates agreed to within 10% on the hemispheres and on the sphere-cone forebodies, and to within 10% in CO_2 and 25% in air on the afterbodies and stings of the sphere-cone models.

NOMENCLATURE

C_H	Stanton number, $q/[\rho_4 u_4 (h_{tot} - h_w)]$
h	enthalpy (J/kg)
k	thermal conductivity (W/m-K)
M	Mach number
p	pressure (N/m^2)
q	heat transfer rate (W/m^2)
R	radius (m)
Re	Reynolds number
S	distance along model surface (m)
T	temperature (K)
t	time (sec)
U_∞	freestream velocity (m/sec)
y_{ref}	reference length (m)
α	thermal diffusivity (m^2/sec)
β	thermal product, $\alpha/\sqrt{k}$ (W-sec$^{1/2}$/m^2-K)
λ	correction factor (1/K)
σ	heat transfer residual
ρ	density (kg/m^3)
τ	non-dimensional time, $\tau = U_4 \Delta t_{est} / y_{ref}$

Subscripts:

∞	freestream
w	wall
tot	total

INTRODUCTION

The NASA HYPULSE Expansion Tube[1], which is operated by the General Applied Sciences Laboratories of Long Island, New York (HYPULSE was previously operated by the NASA Langley Research Center), is an impulse facility in which hypervelocity, high-enthalpy flows can be produced using a variety of test gases. HYPULSE is used in the study of high-temperature, chemically-reacting internal and external flows, such as that inside a scramjet[2] or around a planetary entry vehicle[3]. Data from these studies can match or be extrapolated to flight conditions, or can be employed in the validation of computational fluid dynamics codes.

In this work, heat-transfer measurements were made in HYPULSE on 70 deg sphere-cone entry vehicle configuration models and on hemispheres of various radii. The hemisphere tests were conducted in order to assess the performance of the HYPULSE facility, while the sphere-cone model tests were conducted in order to obtain data for comparison with computational results.

---

* Graduate Researcher, AIAA Member

† Professor, Mechanical and Aerospace Engineering Dept., Associate Fellow AIAA

FACILITY DESCRIPTION

The HYPULSE Expansion Tube (Fig. 1) has an internal diameter of 15.24 cm, length of 30 m, and is divided into three sections: driver, intermediate (driven) and acceleration. The driver section is filled with highly pressurized helium gas, and is separated by a steel double-diaphragm from the lower-pressure intermediate section, which is filled with the desired test gas. A Mylar diaphragm divides the intermediate section from the acceleration section, which is filled with test gas at even lower pressure. A HYPULSE run is initiated by bursting the steel double diaphragms, which produces a supersonic shock-tube flow in the intermediate section. When the incident shock wave reaches the end of the intermediate section, the Mylar diaphragm bursts, and a high-enthalpy, hypersonic flow is produced as the test gas expands into the acceleration section. Models are positioned at the end of the acceleration section, where the expansion tube exits into an enclosed test section. This operating sequence is represented by the distance-time (XT) diagram in Fig. 2.

This expansion tube mode of operation is unique in that a high-enthalpy flow is produced with a freestream which is virtually free of chemical dissociation. This is in contrast to reflected shock tunnels, in which the flow is stagnated and then processed by a shock wave in order to generate the desired high enthalpy and velocity. This produces a high-enthalpy flow which has a greater test time than an expansion tube flow, but does so at the expense of some test-gas dissociation.

TEST CONDITIONS

HYPULSE has a variety of operating points in which air, CO_2, He, N_2 or O_2 can be employed as test gases. In this study, operation of HYPULSE was limited to the conditions listed in Table 1, which are referred to as "the Langley conditions" as they are derived from those at which the facility was operated when it was operated by the Langley Research Center. Conclusions drawn in this paper should be interpreted as referring only to those conditions, and not to the overall capabilities of the HYPULSE Expansion Tube.

Detailed calibration studies have been performed at the Langley conditions[4]. For both air and CO_2, pitot pressure surveys at the exit of the expansion tube have identified an inviscid test core of approximately 3 in. diameter over which the pitot pressure is constant to within ±6%. At the Langley conditions, nominal steady-flow test times have been determined from pitot and tube wall pressure data to be on the order of 250 μsec.

In this work, the steady-flow test period of each run was determined by examination of wall pressure data (the presence of the test model left no room for a pitot probe). Because surface heating rates were observed to be very sensitive to variations in the freestream conditions, a small acceptable magnitude of deviation in the wall pressure was stipulated, and consequently the accepted test durations were shorter than the nominal times. Typical wall-pressure time-histories for CO_2 and air runs are shown in Figs. 3 and 4. To determine the steady-state run duration, the wall pressure was first averaged over a 100 μsec interval centered 150 μsec from the arrival of the incident shock wave for CO_2 or 200 μsec from the incident shock wave for air. The total test period was then taken to be the time over which the wall pressure varied by no more than ±5% from the average value over the 100 μsec interval. Based on the application of this criterion to all of the CO_2 and air runs conducted in this research, the average steady-state run duration for heat-transfer testing at the Langley conditions was found to be 150 μsec for CO_2 and 125 μsec for air. These values are more conservative than the quoted nominal values, but as the heating data were intended for comparison with computational results, the ±5% pressure deviation criteria was imposed in order to minimize the uncertainty in the freestream flow conditions.

The flow conditions for each run were computed using the Equilibrium Reacting Gas (ERGAS) code[5]. Inputs required for this code are the freestream velocity, the pitot pressure and the freestream static pressure. The freestream velocity was assumed to be equal to the incident shock velocity, which was computed for each run from the time required for the pressure disturbance caused by the incident shock to travel between wall pressure stations in the expansion tube. The freestream pressure was assumed to be equal to the time-averaged wall pressure measured immediately upstream of the end of the expansion tube, while the pitot-pressure was computed from wall-pressure to pitot-pressure calibrations[6]. The test conditions in Table 1 represent the average of the conditions computed using ERGAS for all of the runs in this study (26 in CO_2 and 20 in air). Uncertainty estimates for the run-to-run repeatability of test flow

conditions are also given in Table 1. The uncertainties are estimated by two standard-deviations of the individual properties from their average values, where the standard deviations are computed statistically from the data from all the runs. Flow properties were found to be quite repeatable in this test series. In both test gases the greatest uncertainty was in the freestream pressure, which was estimated to be ±10%, while the freestream density and velocity uncertainties were estimated to be no more than ±3%.

HEAT-TRANSFER MODELS

Heat-transfer models of the two geometries studied in this work, a hemisphere and a 70 deg sphere-cone, were machined from Macor ceramic. Glass or ceramic materials such as quartz, pyrex or Macor are commonly used in the construction of heat-transfer models because they are thermal insulators, and thus the thermal penetration depth into a model fabricated from one of these materials is small. Because of this, a greater, and thus more easily measured, surface temperature rise is produced on the surface of the model. Furthermore, the substrate can be treated as being of semi-infinite thickness: that is, the thermal penetration depth of the heat load into the substrate is much less than the thickness of the model wall. This semi-infinite substrate assumption is required in the development of several of the methods commonly employed for the computation of surface heating rates from measured temperature time-history data. Macor was chosen as the model material over quartz or pyrex in this work because it is more easily machined than quartz, and because it exhibits smaller variations in thermal properties with temperature than pyrex.

Models were instrumented with thin-film temperature resistance gages (following the procedure described in Ref. 7), which were used to measure temperature time-histories on the models' surfaces. A thin-film gage is an approximately 1000 Å thick palladium sensing element which is applied to a model either through a mechanical deposition process or by hand-painting. Approximately 95% of the gages in this study were applied through the deposition process; gages were hand-painted only in regions of extreme surface curvature, such as the corners of the sphere-cone models, were deposition was impractical. Typical gage resistances were on the order of 100-150 Ω. Gages were coated with a thin layer of aluminum dioxide (Al_2O_3) to protect them from electrical shorting due to any ionization in the acceleration gas. Note that the combined thickness of the sensor and overlayer was much less than the thermal penetration depth into the substrate, and therefore it could be assumed that they had a negligible effect on the heat transfer to the model.

Hemisphere models of three different radii, 1/4 in., 3/8 in. and 1/2 in. were built for use in this study. The hemisphere models were supported on stainless-steel stings of radii equal to the hemisphere. A sting-adapter capable of a supporting a sting and model of each of the three radii was fabricated so that the 1/4 in., 3/8 in. and 1/2 in. models could be tested simultaneously. The 70 deg sphere-cone models (Fig. 5) had a forebody base radius of 1 in., nose-to-base radii ratio of 0.5, and a 0.05 corner-to-base radii ratio. The sphere-cone models also had a 40 deg cone-frustrum afterbody with a 0.6 frustrum-to-base radius ratio. Each 70 deg sphere-cone model was equipped with a 0.406 in. radius sting which had a contoured Macor insert with additional thin-film gages. The sting was fitted to a 45 deg cone strut-adapter. The adapter was mated to the sting at a point 4.6 forebody base radii downstream from the frustrum, which was a sufficient distance to ensure that boundary layer separation induced by the shock at the adapter would not influence the near-wake region of interest directly behind the model.

The 1/4 in., 3/8 in. and 1/2 in. radii hemispheres were instrumented with 1, 9, and 17 thin-film gages, respectively, along a single arc through the hemispheres' stagnation points. The 70 deg sphere-cone models each carried 37 thin-film gages, while the Macor inserts on their stings had an additional 33 thin-film gages. This produced a surface spacing of approximately 0.1 in., and provided a continuous line of instrumentation covering the forebody, afterbody and model sting. (Fig. 6).

The gages on the sphere-cone models were destroyed at the end of each run by the high-pressure driver gas and debris from the diaphragms. Therefore, several uninstrumented stainless-steel 70 deg sphere-cone models were fabricated and tested on the instrumented stings in order to gather further wake data without the time and expense of building additional instrumented Macor models.

DATA ACQUISITION AND REDUCTION

Data acquisition in the HYPULSE Expansion Tube is performed with a LeCroy™ Model 6810 Waveform Digitizer, which is capable of processing 152

channels of data, of which 10 are reserved for facility use. For aerothermodynamic testing, thin-film gage current is supplied by LAMBDA™ type LQ411 low-noise linear power supplies through GASL manufactured, 20-channel, floating ground-point gage control units. In these tests, gage current was supplied at a constant 1 mA, which was sufficient to minimize ohmic heating of the gages. The data sampling rate for the present work was 500 kHz.

Test data were in the form of voltage time-histories for each of the thin-film gages, which were converted to temperature time-histories using prior voltage-temperature calibrations and gage resistance measurements. The temperature time-histories were then input into the 1DHEAT data reduction code[8], which was used to compute the heat-transfer rates.

Three different data reduction schemes, all of which are based on the assumption of one-dimensional heat conduction[9] into the model substrate, are incorporated into the 1DHEAT code. The first two, the classic Cook-Felderman technique[10] and the related Kendall-Dixon technique[11,12], are analytical methods in which the assumptions of heat conduction to a semi-infinite solid with constant thermal properties are used to derive closed-form solutions for the heating rates. The third technique is a numerical solution of the one-dimensional finite-volume heat-conduction problem.

In the Cook-Felderman method, which is also referred to as the direct method, the heat-transfer rate is computed from the temperature-time history via:

$$q(t_n) = \frac{2\beta}{\sqrt{\pi}} \sum_{i=1}^{i=n} \frac{T_i - T_{i-1}}{\sqrt{t_n - t_i} + \sqrt{t_n - t_{i-1}}} \qquad (1)$$

In the Kendall-Dixon method, which is also referred to as the indirect method, the total heat energy added to the model is first computed from:

$$Q(t_n) = \frac{\beta}{\sqrt{\pi}} \sum_{i=1}^{n} \frac{T_i + T_{i-1}}{\sqrt{t_n - t_i} + \sqrt{t_n - t_{i-1}}} \Delta t \qquad (2a)$$

The time history of the heat-transfer rate is then computed as:

$$q(t_n) = \frac{dQ_n}{dt} = \frac{-2Q_{i-8} - Q_{i-4} + Q_{i+4} + 2Q_{i+8}}{40\Delta t} \qquad (2b)$$

Over a given time interval, both direct and indirect method computations will yield nearly identical time-averaged values. However, the instantaneous heating rates are quite different due to the fact that the wide four-point differencing stencil in Eq. (2b) tends to dampen fluctuations in the time history. This is illustrated in Fig. (7). While this is useful for reducing experimental noise, this method would not be recommended if transient phenomena such as turbulence were of interest. The indirect method was preferred in this work because only the steady-state heating rates (or quasi-steady in regard to the flow establishment process) were of interest.

Both Eqs. (1) and (2) were derived with the assumption of constant material thermal properties. However, materials commonly used in the construction of heat-transfer models, such as quartz, pyrex, or in this case Macor, do exhibit a dependence of thermal properties on temperature. Thus, because of the high temperatures produced in a model exposed to a hypersonic flow, direct application of these methods will result in large errors. To deal with this problem, an empirical correction factor for the effects of thermal properties was derived[8] which has the form:

$$q_{var} = q_{const}\left(1 + \lambda \Delta T_w\right) \qquad (3)$$

where λ is the correction factor, ΔT_w is the increase in surface temperature from ambient room temperature, and q_{const} is the value computed using either Eq. (1) or Eq. (2). The correction factor is given by:

$$\lambda = 7.380 \times 10^{-4} - 4.604 \times 10^{-7}\, \Delta T_w \qquad (4)$$

This empirical method has proven to be very accurate, and is useful for rapid real-time analysis of experimental data. However, for a more rigorous analysis of heating data, a numerical solution of the one-dimension heat conduction equation should be preformed. In 1DHEAT, a numerical solution is computed via an implicit, one-dimensional, finite-volume technique. In a numerical solution, the semi-infinite assumption is not required, and the variation of thermal properties with temperature can be accounted for directly. Boundary conditions for the numerical solution are the measured surface-temperature time-history on the exterior of the model and an adiabatic boundary at the interior of the model. Note that the correction factor in Eq. (3) for the analytical methods was derived by comparison of constant-properties solutions from Eqs. (1) and (2) to finite-volume

solutions. In this study, the indirect method was used for initial analysis of the data during testing, and the finite-volume method was used to verify these results after the test series was completed.

In order to minimize experimental noise, final values of the surface heat-transfer rates for the hemispheres and 70 deg sphere-cone model forebodies were computed by time-averaging the data over the steady-flow window determined from examination of the wall pressure time history data. However, the analysis of the heating data from the afterbody and model sting was somewhat more complicated due to the transient nature of the flow establishment process. While the forebody flow establishment process is fairly rapid (~50 μsec), the time required for the flow in the wake of a blunt body, such as the 70 deg sphere-cone configuration, can amount to a significant fraction of the total test time available in an impulse facility. During this establishment process, there are large fluctuations in both the magnitude and the shape of the wake heating distributions. It is therefore necessary to determine at what point the wake flow field has become fully established in order to determine the time-interval over which to average the heating rates.

In order to determine when the wake flow could be considered as established, an establishment criterion based on the change in the measured heat-transfer rates between sample times was defined[13]. For an individual gage, this heat-transfer "residual" is defined by:

$$\sigma(t) = \frac{\Delta q\,(t)}{q\,(t)} \tag{5}$$

In order to characterize the entire wake region, the root-mean-square (RMS) variation of all the wake gages is computed at each sample time by:

$$RMS(\sigma) = \sqrt{\frac{1}{n}\left(\sigma_1^2 + \sigma_2^2 + \ldots \sigma_n^2\right)} \tag{6}$$

The time-history of the RMS can be used to identify the established flow period and to locate the arrival time of features of the expansion tube wave system, as shown in Fig. 8. Based on examination of time-histories of both the heat-transfer rates and the overall heat-transfer distributions, it was concluded that the wake flow could be considered to be established when the RMS had dropped below a value of ~0.02. In regard to the use of Eq. (6), it should be pointed out that heat-transfer gages which have gone "bad" (i.e. those that return an extremely noisy signal) should not be included in the RMS computation or the results will be skewed by the noise from these gages.

The RMS criteria was applied to each run and a non-dimensional flow establishment time for the 70 deg sphere-cone wake flow was calculated from:

$$\tau = \frac{U_4 \Delta t_{est}}{y_{ref}} \tag{7}$$

In Eq. (6), Δt_{est} is defined as the time from the arrival of the incident shock, and y_{ref} is defined as the difference between the forebody radius and the sting radius. τ varied from 45 to 75 with an average value of 60 in the CO_2 tests, and varied from 60 to 90 with an average value of 70 in the air tests. These values are consistent with previous studies[14], and represent for either gas approximately 75% of the total time from the arrival of the incident shock to the end of the test period.

MATERIAL PROPERTIES

The finite-volume technique provides a more theoretically sound means of performing heat transfer computations than the analytical techniques with their empirical corrections. However, the lack of adequate information on material thermal properties presents practical difficulties regardless of the method employed. Thermal properties information in aerospace literature is not well documented and is often contradictory. A collection of references for thermal properties of different materials, as well as suggested values for thermal properties, is presented in Ref. 8. It is possible by using data from different sources listed therein to calculate heat-transfer rates which vary by more than 20%. It thus should be obvious that this is an area of concern and that more research into the thermal properties of common model substrate materials must be conducted.

At present, the following curve fits for Macor thermal properties for temperatures up to 600 K are recommended:

$$\rho = 2543.84 \quad (\mathrm{kg/m^3}) \tag{8}$$

$$k = 0.33889 + 7.4682 \times 10^{-3} T - 1.6118 \times 10^{-5} T^2 + 1.2376 \times 10^{-8} T^3 \quad (\mathrm{W/m-K}) \tag{9}$$

$$\alpha = 1.3003 \times 10^{-6} - 2.2523 \times 10^{-9} \times T + 1.8571 \times 10^{-12} \times T^2 \quad (m^2/s) \tag{10}$$

The validity of these curve fits was assessed in tests on a 2 in. diameter Macor hemisphere in the LaRC 31-Inch Mach 10 Air Tunnel, a facility in which chemical reactions are not a concern because of the low total enthalpy levels, and which is known for its high flow uniformity[15]. Stanton numbers computed from heat-transfer measurements were compared to both viscous-shock layer (VSL) calculations (courtesy of Roop Gupta, NASA LaRC) and Stanton numbers values measured on an identical quartz hemisphere which was tested simultaneously with the Macor hemisphere. These values are all normalized by the stagnation-point Stanton number computed using the Fay-Riddell[16] method. As seen in Fig. 9, the Macor hemisphere results are within 5% of both the quartz and VSL values, as well as the Fay-Riddell value. That suggests that these curve fits are reasonably accurate at least up to the stipulated temperature limit.

EXPERIMENTAL RESULTS

Heat-transfer rates computed from temperature time-history data for the hemisphere tests are given in Fig. 10 for CO_2 and Fig. 11 for air. For each test gas, two runs were made in which each of the three radii models were simultaneously tested. Heating rates were found to be repeatable to within less than ±5%, and as shown in Fig. 12, the stagnation-point values followed the theoretically predicted inverse linear variation with the square-root of the hemisphere radius.

Heat-transfer data from the 70 deg sphere-cone tests are presented in Fig. 13 for CO_2 and Fig. 14 for air. Several runs were made in each test gas with both instrumented and uninstrumented sphere-cone models on fully instrumented stings. Afterbody and sting heat-transfer rates were an order of magnitude lower than on the forebody. Peak wake heat-transfer rates occurred approximately 1.5 forebody radii down the sting from the model (the sting begins at $S/R_b = 1.91$), and were equal to approximately 5% of the forebody stagnation-point values for tests in both gases.

The experimental measurement uncertainty was estimated by two standard deviations of the heating measurements made during the steady test-flow period. This estimate of the uncertainty gave values of approximately ±10% of the mean values on the forebody and ±15% on the afterbody and sting.

Measured heat-transfer rates were compared to predictions made using NEQ2D[17], a 2D/axisymmetric non-equilibrium Navier-Stokes solver. Freestream conditions for the computational solutions were taken from Table 1. Owing to the short duration of a HYPULSE test, the surface temperature rise on a test model was negligible with respect to the total temperature (6028 K in air, 3703 K in CO_2), and so the surface heating rates remained essentially constant. Therefore, a uniform 300 K surface temperature distribution was specified for the computations. Also, the Macor from which the test models were machined was considered to be non-catalytic surface.

Comparisons for the 1/2 in. radius hemisphere models are shown in Figs. 15 and 16. In the CO_2 tests, the computed heat-transfer rates were approximately 5% higher than the experimental data. For the air tests, the computed values were approximately 7% higher than the experimental data.

Comparisons for the 70 deg sphere cone models are presented in Figs. 17 and 18. Note that the forebody and sting heating rates are shown on separate y-axes in order to emphasize the details in both regions. Computed forebody heat-transfer rates were within 7% of the experimental data in CO_2 and within 10% in air. Computed sting heating values in CO_2 were within 10% of the experimental data except in the region immediately behind the model, where a larger discrepancy occurred. Values for air were within 25% all along the sting, although the rates were over-predicted in the recirculation region, and under-predicted in the peak-heating region.

SUMMARY AND CONCLUSIONS

The capability for performing high-enthalpy, hypervelocity aerothermodynamic studies in the HYPULSE Expansion Tube has been demonstrated in tests on hemisphere and 70 deg sphere-cone Macor heat-transfer models in both CO_2 and air. The run-to-run variations in freestream flow conditions were between ±3% and ±10% for the individual properties, and the average steady-freestream test period was found to be 150 μsec in CO_2 and 125 μsec in air. Heat-transfer measurement uncertainty was estimated to be no more than ±10% on the hemisphere models and on the forebodies of the sphere-cone models. Sphere-cone wake flow establishment required on the order of 60

flow-path lengths in CO_2 and 70 in air, and the wake heat-transfer uncertainty was estimated to be no more than ±15%. Navier-Stokes computations were found to agree with the experimental data to within 10% in CO_2 and 25% in air for the wake heating rates. For the hemispheres and 70 deg sphere-cone forebodies, agreement was within 10% in air and 7% in CO_2.

ACKNOWLEDGMENTS

This research was funded under grants NAGW-1331 and NAG1-1663 to North Carolina State University. Funding for model fabrication and testing in HYPULSE was provided by the Aerothermodynamics Branch, NASA Langley Research Center. The authors wish to thank John Calleja of GASL for his assistance in this work and Graham Candler of the University of Minnesota for the use of the NEQ2D code.

REFERENCES

(1) Tamagno, J., Bakos, R., Pulsonetti, M., and Erdos, J., "Hypervelocity Real Gas Capabilities of GASL's Expansion Tube (HYPULSE) Facility," AIAA Paper 90-1390, June 1990.

(2) Bakos, R., Tamagno, J., Rizkalla, O., Pulsonetti, M., and Chinitz, W., "Hypersonic Mixing and Combustion Studies in the GASL HYPULSE Facility," AIAA Paper 90-2095, June 1990.

(3) Calleja, J., Trucco, R., Tamagno, J., and Erdos, J., "Results of Hypervelocity Aeroheating Tests of Aeroassist Flight Experiment (AFE) Forebody Models in Air, Helium, and CO_2," GASL TR 326, Oct. 1990.

(4) Calleja, J., Tamagno, J., and Erdos, J., "Calibration of the GASL 6-Inch Expansion Tube (HYPULSE) for Air, Helium, and CO_2 Test Gases," GASL TR 325, Sept. 1990.

(5) Miller, C. G., "Computer Program of Data Reduction Procedures for Facilities using CO_2-N_2-O_2-Ar Equilibrium Real-Gas Mixtures," NASA TMX–2512, March, 1972.

(6) DiFulvio, M., NASA Langley Research Center. Private communication, 1994.

(7) Miller, C. G., "Comparison of Thin-Film Resistance Heat-Transfer Gages with Thin-Skin Transient Calorimeter Gages in Conventional Hypersonic Wind Tunnels," NASA TM 83197, Dec., 1981.

(8) Hollis, B. R., "User's Manual for the One–Dimensional Hypersonic Aero-Thermodynamic (1DHEAT) Data Reduction Code," NASA CR 4691, August, 1995.

(9) Schultz, D. L. and Jones, T. V., "Heat Transfer Measurements in Short-Duration Hypersonic Facilities," AGARD-AG-165, February, 1973.

(10) Cook, W. J. and Felderman, E. J., "Reduction of Data from Thin-Film Heat Transfer Gages: A Concise Technique," AIAA Journal, Vol 4. No. 3, March 1966, pp. 561-562.

(11) Kendall, D. N., Dixon, W. P., and Schulte, E. H., "Semiconductor Surface Thermocouples for Determining Heat-Transfer Rates," IEEE Transactions on Aerospace and Electronic Systems, Vol. AES-3, No. 4, July, 1967, pp. 596-603.

(12) Hedlund, E. R., Hill, J. A. F., Ragsdale, W. C., and Voisinet, R. L. P., "Heat Transfer Testing in the NSWC Hypervelocity Wind Tunnel Utilizing Co-axial Surface Thermocouples," NSWC MP 80-151, March 1980.

(13) Hollis, B.R. and Perkins, J. N., "Hypervelocity Aeroheating Measurements in Wake of a Mars Mission Entry Vehicle," AIAA Paper 95-2314, June 1995.

(14) Holden, M. S., "Development and Code Evaluation Studies in Hypervelocity Flows in the LENS Facility," 2nd European Symposium on Aerothermodynamics for Space Vehicles, ESTEC, Noordwijk, The Netherlands, Nov., 1994.

(15) Micol, J.R., "Hypersonic Aerodynamic /Aerothermodynamic Testing Capabilities at Langley Research Center: Aerothermodynamic Facilities Complex," AIAA Paper 95-2107, 1995.

(16) Fay, J. A., and Riddell, F. R., "Theory of Stagnation Point Heat Transfer in Dissociated Air," J. Aero. Sci., vol. 25, no. 2, Feb, 1958, pp. 73-85.

(17) Candler, G. V., "Computation of Thermo-Chemical Nonequilibrium Martian Atmospheric Entry Flows." AIAA Paper 90-1695, June 1990.

Table 1. HYPULSE Flow Properties at Langley Test Conditions

Test Gas	P_∞ (Pa)	T_∞ (K)	ρ_∞ (kg/m^3)	$P_{0,2}$ (Pa)	U_∞ (m/s)	M_∞	$h_{tot} - h_{298K}$ (MJ/kg)
CO_2	1187±10.8%	1088±8.7%	0.005789±3.1%	129,600±1.8%	4772±1.1%	9.71±4.1%	12.25±2.1%
Air	1824±9.9%	1113±9.3%	0.005712±1.8%	147,200±1.3%	5162±0.9%	7.93±4.1%	14.18±1.4%

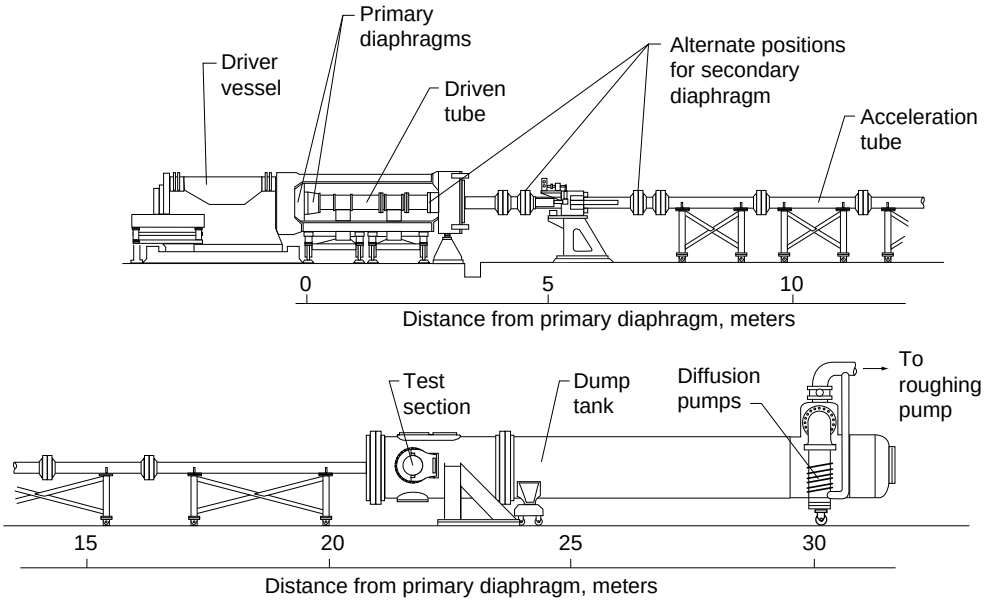

Figure 1. HYPULSE Expansion Tube

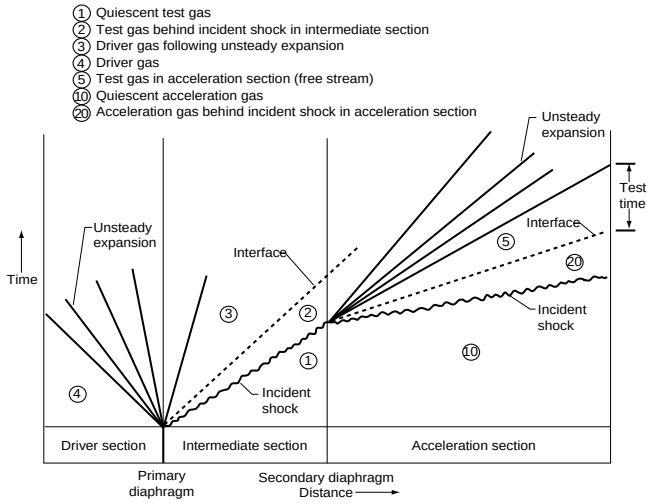

Figure 2. XT Diagram

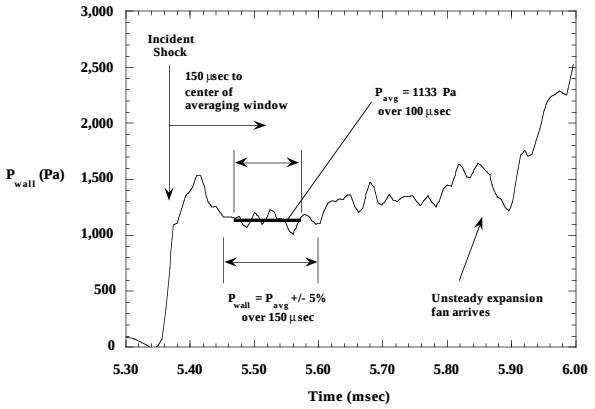

Figure 3. Typical Wall Pressure for CO_2 Test

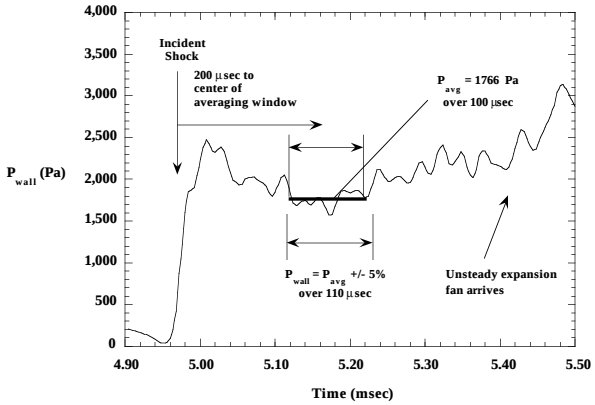

Figure 4. Typical Wall Pressure for Air Test

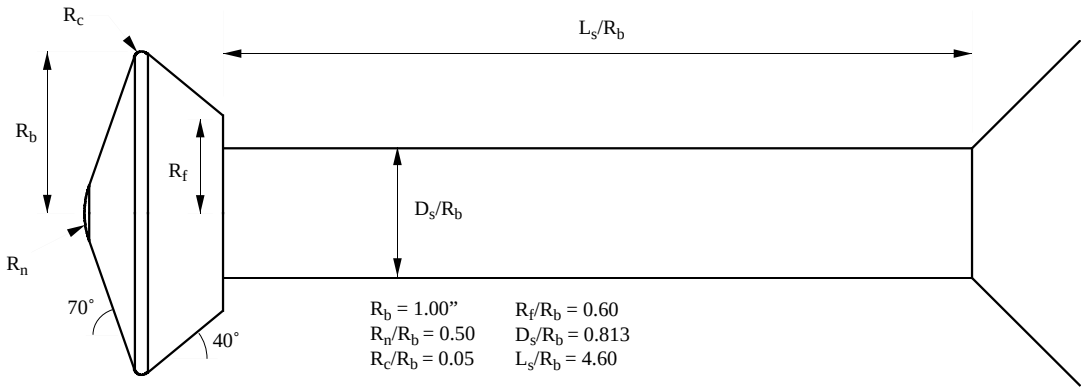

Figure 5. 70 Deg Sphere-Cone and Sting Dimensions

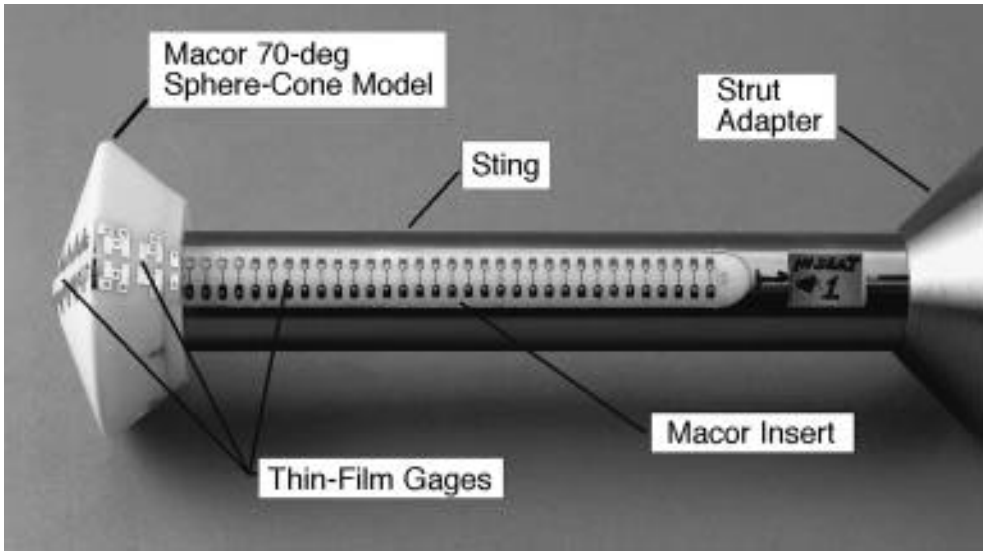

Figure 6. 70 deg Sphere-Cone and Sting Gage Layout

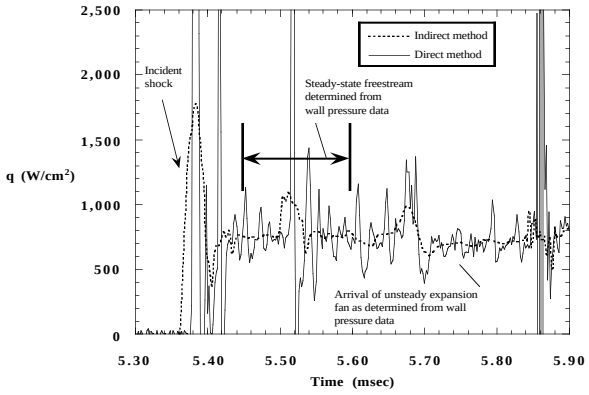

Figure 7. Comparison of Heat-Transfer Rates from Direct and Indirect Methods

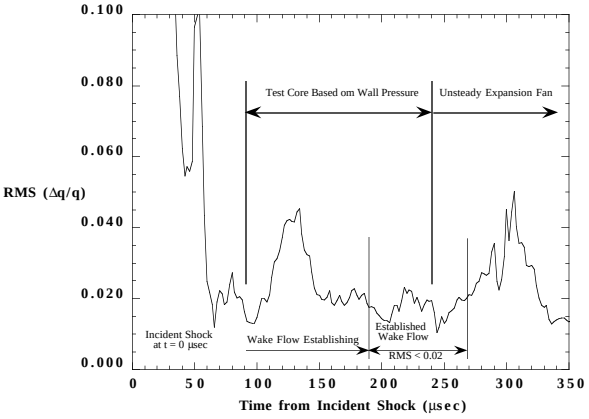

Figure 8. Wake RMS Time History for CO_2 Test

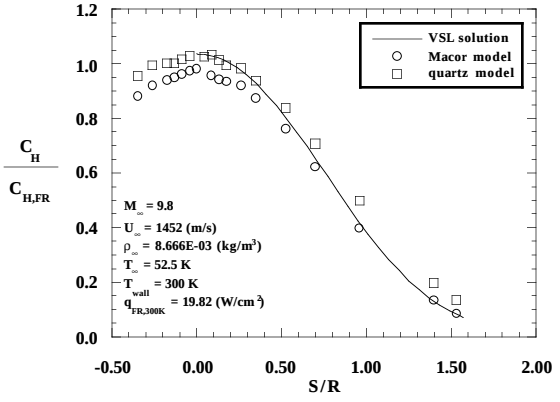

Figure 9. Measured Heating on 1/2 in. rad. Macor and Quartz Hemispheres vs. VSL Computations, NASA LaRC 31-Inch Mach 10 Air Tunnel

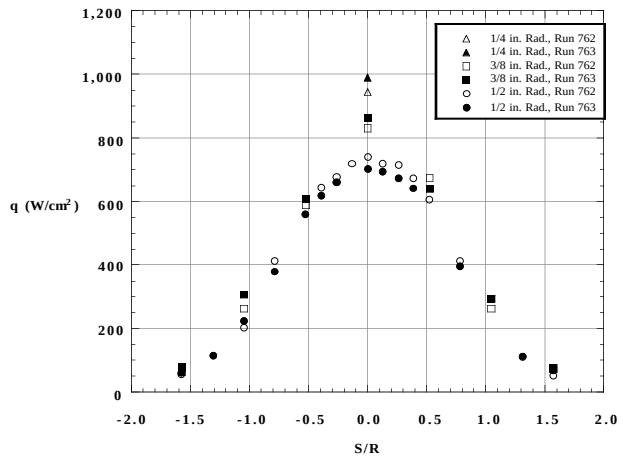

Figure 10. Hemisphere Heating in CO_2

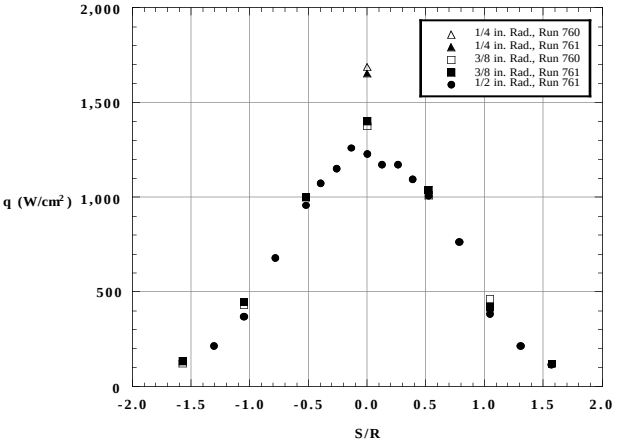

Figure 11. Hemisphere Heating in Air

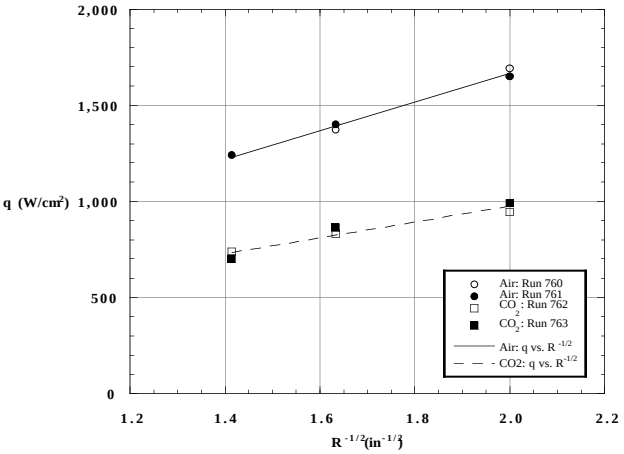

Figure 12. Hemisphere Heating Correlation

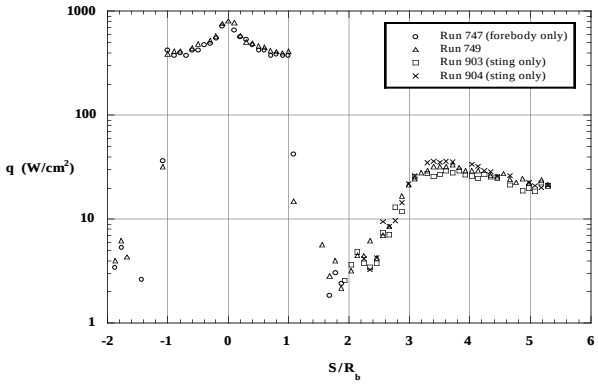

Figure 13. 70 Deg Sphere-Cone Heating in CO_2

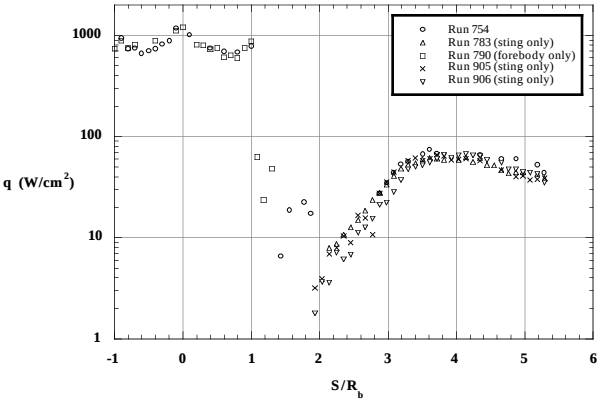

Figure 14. 70 Deg Sphere-Cone Heating in Air

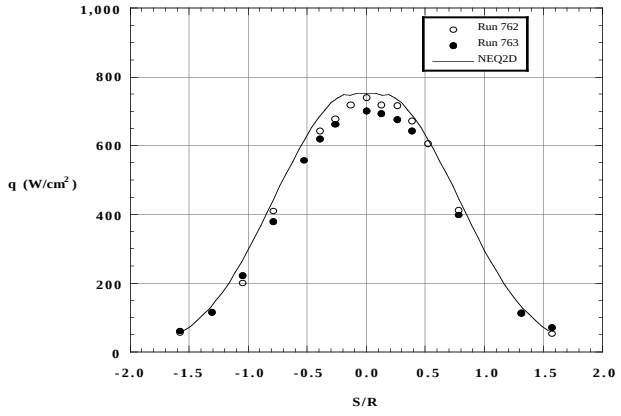

Figure 15. Computations vs. Experimental Data for 1/2 in. Radius Hemisphere in CO_2

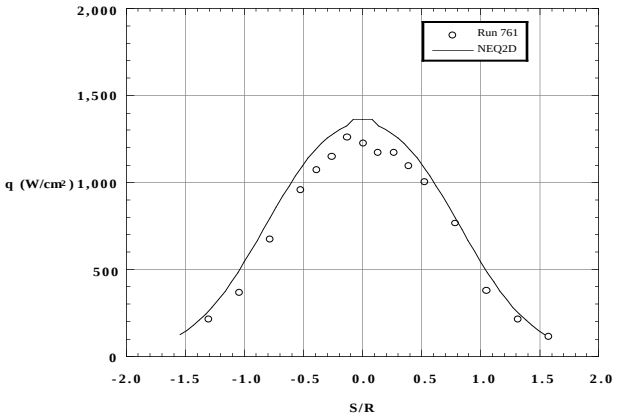

Figure 16. Computations vs. Experimental Data for 1/2 in. Radius Hemisphere in Air

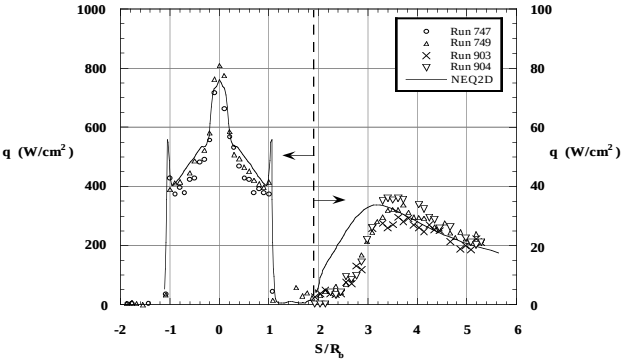

Figure 17. Computations vs. Experimental Data for 70 Deg Sphere-Cone in CO_2

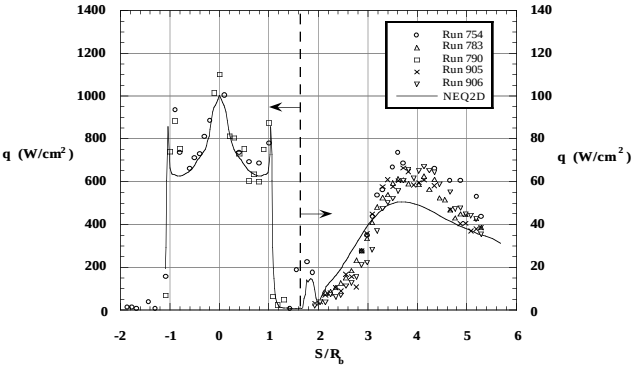

Figure 18. Computations vs. Experimental Data for 70 Deg Sphere-Cone in Air